A Generalized Procedure for the Prediction of Multicomponent Adsorption Equilibria

Austin Ladshaw, Sotira Yiacoumi, and Costas Tsouris
School of Civil and Environmental Engineering, Georgia Institute of Technology, Atlanta, GA 30332

DOI 10.1002/aic.14826
Published online April 27, 2015 in Wiley Online Library (wileyonlinelibrary.com)

Prediction of multicomponent adsorption equilibria has been investigated for several decades. While there are theories available to predict the adsorption behavior of ideal mixtures, there are few purely predictive theories to account for nonidealities in real systems. Most models available for dealing with nonidealities contain interaction parameters that must be obtained through correlation with binary-mixture data. However, as the number of components in a system grows, the number of parameters needed to be obtained increases exponentially. Here, a generalized procedure is proposed, as an extension of the predictive real adsorbed solution theory, for determining the parameters of any activity model, for any number of components, without correlation. This procedure is then combined with the adsorbed solution theory to predict the adsorption behavior of mixtures. As this method can be applied to any isotherm model and any activity model, it is referred to as the generalized predictive adsorbed solution theory. © 2015 American Institute of Chemical Engineers *AIChE J*, 61: 2600–2610, 2015
Keywords: adsorption, multicomponent, equilibrium, isotherm, nonideal

Introduction

Adsorption isothermal equilibrium has been the cornerstone of adsorption modeling and separation process design for decades. For simple, single-component systems, it is generally sufficient to represent adsorption equilibria in terms of a series of isotherms. This type of data describes the equilibrium partition between the gas and solid phases at a constant temperature. A series of isotherms, each at a different temperature, would then allow for interpolation of the adsorption equilibrium behavior expected at any temperature and pressure that falls within that applicable temperature range. In real separation processes, however, there are multiple gas species involved. Therefore, one needs to be capable of predicting how each species would behave and interact with other species and the adsorbent surface. To accomplish this feat, proposed here is a procedure, which can be utilized in the prediction of multicomponent adsorption equilibria for any number of gas species. The aim is to provide a theory that is general enough to allow other scientists and engineers to extend the basic ideas developed in this work by simply applying different isotherm and activity models.

One of the most well-known multicomponent adsorption theories is the adsorbed solution theory (AST) proposed by Myers and Prausnitz and shown below in Eqs. 1 through 6.[1]

$$\Pi = \frac{\pi A}{RT} = \int_0^{p_i^o} \frac{q_i^o}{p_i^o} dp_i^o \tag{1}$$

$$P_T y_i = p_i^o x_i \gamma_i \tag{2}$$

$$q_T = \left[\sum_{i=1}^{N} \frac{x_i}{q_i^o} + \sum_{i=1}^{N} x_i \left(\frac{\partial \ln \gamma_i}{\partial \Pi} \right)_{T,x} \right]^{-1} \tag{3}$$

$$\sum_{i=1}^{N} x_i = 1 \tag{4}$$

$$q_i = q_T x_i \tag{5}$$

$$q_i^o = f(p_i^o) \tag{6}$$

This theory was derived from the Gibbs thermodynamic expression for physical adsorption and assumes that the adsorbent is thermodynamically inert and contains a specific surface area (A) that is shared by all adsorbates. Intensive properties of the system are temperature (T), spreading pressure (π), and adsorbed phase composition (x_i, x_j, …, x_N) while the extensive property of the mixture is the total surface loading (q_T).[1]

For any given mixture, the surface energy per unit area (i.e., spreading pressure) must be a constant. Therefore, it is often lumped into a combined spreading pressure term (Π) for convenience. Additionally, as this term is constant for the mixture, each pure species isotherm integral (Eq. 1) must evaluate to the same value, which places a constraint in the system of equations. To obtain the pure species (i.e., reference state) pressure (p_i^o), Raoult's Law is applied between

Correspondence concerning this article should be addressed to S. Yiacoumi at sotira.yiacoumi@ce.gatech.edu.

the gas and solid phases (Eq. 2), which couples the activity (γ_i) and adsorbed mole fraction (x_i) to the gas phase partial pressure ($P_T y_i$).[1]

The primary advantage of AST was that it allowed for the prediction of the mixed gas adsorption equilibria for any pure gas isotherm, $q_i^o = f(p_i^o)$. Furthermore, if the adsorbed phase was assumed to behave like an ideal solution, then the activity coefficients for each species would be equal to one ($\gamma_i = 1$, for all i). This simplification made the system of equations solvable and could then be used to predict adsorption equilibria for any number of components (N).

Unfortunately, the assumption of ideality in the adsorbed phase has been shown to produce fairly large errors, when the model is compared against experimental data.[2–4] Largely, these errors are attributed to the activity coefficients, though other explanations suggest they may stem from surface heterogeneity of the adsorbents.[4,5] Either way, it has become common practice to propose various activity models to account for the nonideality of real-mixed gas systems. Some models that have been utilized include the Flory-Huggins[6] and Wilson[7] equations, as well as the UNIQUAC[8,9] and UNIFAC[10] models. However, all these models lack a relationship between the spreading pressure (π) and activity coefficient (γ_i) as Eq. 3 above requires.

In order for an activity model to be considered thermodynamically consistent, it must abide by three criteria[2,3] detailed below in Eqs. 7 through 9

$$\lim_{x_i \to 1} \gamma_i = 1 \tag{7}$$

$$\lim_{\pi \to 0} \gamma_i = 1 \tag{8}$$

$$\lim_{x_i \to 0} \gamma_i = \gamma_i^{\infty} \tag{9}$$

Equation 7 states that the activity of a particular component must become unity, when the adsorbed mole fraction (x_i) of that component approaches one. In addition, the activity must also approach unity as the spreading pressure approaches zero. When the mole fraction of a component approaches zero in the adsorbed phase, then there is some infinite dilution activity (γ_i^{∞}) attained,[11] which usually displays a negative deviation from Raoult's Law.[5]

Unlike the other activity models mentioned above, the spreading pressure dependent (SPD) model proposed by Talu and Zwiebel[3] and shown below in Eqs. 10 through 14, does abide by the thermodynamic criteria in Eqs. 7 through 9

$$\ln \gamma_i = s_i \left[1 - \ln\left(\sum_{j=1}^{N} \theta_j \tau_{ji} \right) - \sum_{j=1}^{N} \frac{\theta_j \tau_{ij}}{\sum_{k=1}^{N} \theta_k \tau_{kj}} \right] \tag{10}$$

$$\theta_i = \frac{s_i x_i}{\sum_{j=1}^{N} s_j x_j} \tag{11}$$

$$\tau_{ji} = \exp\left[-\frac{z(e_{ji} - e_{ii})}{2RT} \right] \tag{12}$$

$$e_{ii} = \frac{2(Q_i^{\mathrm{st}} - Q_{i,o}^{\mathrm{st}})}{z s_i} \tag{13}$$

$$e_{ji} = \sqrt{e_{ii} e_{jj}} (1 - \beta_{ji}) \tag{14}$$

This model was developed as an adaptation of the UNIQUAC activity model, and included lateral interaction potentials (e_{ji}) that were related to surface coverage through the difference between the isosteric heat of adsorption (Q_i^{st}) at the spreading pressure of the mixture and the isosteric heat of adsorption at zero spreading pressure ($Q_{i,o}^{\mathrm{st}}$). A quick verification of the SPD model's adherence to Eq. 8 can be shown by recognizing that when the spreading pressure is zero, the interaction potentials all become zero, which in turn causes all the Boltzmann weighting factors (τ_{ji}) to equal one. By substituting this information into Eq. 10, it can be shown that the activity coefficients will always evaluate to unity for zero-spreading pressure. A similar analysis can be performed to verify the SPD model's adherence to Eqs. 7 and 9 as well.

Though the SPD model does stay consistent with the criteria outlined in Eqs. 7 through 9 above, it still contains multiple adjustable parameters, including molecular shape factors (s_i) and a cross-lateral correction parameter (β_{ji}). In that case, an N component mixture will contain a total of $N + N(N-1)/2$ adjustable parameters, which must be determined through binary adsorption experiments.[3] Additionally, as it is impossible to run any adsorption experiments at a constant spreading pressure, it can be extraordinarily difficult to accurately quantify the activities of each species.[5] This drives the need to develop a purely predictive approach to estimating the parameters of the activity model.

In 1998, Sakuth et al. had proposed an extension of AST, called predictive real adsorbed solution theory (PRAST), that intended to estimate the binary interaction parameters of an activity model by looking at the limiting behavior of each component's pure isotherm and using that information to calculate the infinite dilution activities.[11] As a result, each of the pure-component isotherms must obey Henry's Law at low pressure (Eq. 15), which is a thermodynamic expectation for gas adsorption.[2] The infinite dilution activities for each component can then be evaluated from Eq. 16 and combined with the activity model to set up a system of equations in which the adjustable parameters of the model can be explicitly solved for.[11]

$$\lim_{p_i^o \to 0} \frac{q_i^o}{p_i^o} = He_i \tag{15}$$

$$\gamma_i^{\infty}(\pi_j) = \frac{q_j^o(\pi_j)}{He_i p_i^o(\pi_j)} \tag{16}$$

However, this formulation is only valid for a binary mixture because it must be assumed that the adsorbed mole fraction of the other species becomes one ($x_j = 1$) as the mole fraction of the first becomes zero ($x_i = 0$). Additionally, PRAST requires that the activity model itself only have two adjustable parameters for a binary mixture, such as UNIQUAC, in order for the equations to be solvable. Therefore, PRAST would not be applicable for use with SPD because SPD has three adjustable parameters and PRAST only formulates two equations, one for each component.

In an attempt to expand on and overcome the limitations of PRAST, there is a need to modify the SPD model, such that the binary interaction parameters of that model can be determined through the system of equations developed in PRAST. However, modification of SPD alone will not suffice in creating a generalized multicomponent adsorption theory. PRAST itself must also be extended to allow equilibria predictions of mixtures that contain more than just two adsorbable components.

The proposed extension to PRAST is geared toward outlining how one can systematically determine the infinite dilution activities for an N-component mixture, thus, generalizing the

PRAST system into what will be referred to as the generalized predictive adsorbed solution theory (GPAST). Additionally, the lateral interaction potentials of the SPD model will be redefined to allow the model to fit within the GPAST procedure without altering the significance or behavior of the model itself. This reformulated SPD model will be called the modified spreading pressure dependent (MSPD) model. Application of these models and theories will be performed in a computer code developed in C/C++ for the purpose of single component data analysis and multicomponent adsorption predictions. A series of adsorption data from literature will serve as a test case for GPAST. GPAST will then be compared against ideal adsorbed solution theory (IAST) under the same conditions with the intent to demonstrate a significant improvement in predictive capabilities.

Generalized Predictive Adsorbed Solution Theory

In many semipredictive approaches to multicomponent adsorption equilibria, it is common practice to calibrate an activity model for an *N*-component system using binary adsorption data from each unique pair of species in that system.[3,7,8,12] The calibrated parameters of those activity models are then used for the prediction of the ternary and higher systems. However, this calibration approach, based on experimental measurements, is problematic for two main reasons: (i) there is an exponential increase in the number of binary experiments required for calibration as the number of species in a system increases and (ii) it is impossible to carry out adsorption under constant spreading pressure and therefore very difficult to accurately measure the activity of each species in the adsorbed phase.[5]

The principal idea governing GPAST is to predict the parameters of the activity model, without experiments, using each unique binary pair of species within the overall system. By looking at each species pair-wise, as opposed to altogether, the PRAST estimate of the infinite dilution activity (Eq. 16) can be used directly and applied serially to each unique pair. This is now possible because, for a given binary pair, the adsorbed mole fraction of species j will approach unity ($x_j = 1$) as the adsorbed mole fraction of species i approaches zero ($x_i = 0$).

To visualize this concept, consider a system that has three adsorbable species: A, B, and C. In this system, there are three unique binary pairs whose infinite dilution activities must be determined: A + B, A + C, and B + C. Note that the reverse of these pairings (i.e., B + A, C +A, and C + B) is not considered because they are not unique. The infinite dilution activities are determined by Eq. 16 for each species in a pair, such that each pair results in two infinite dilution activities: $\gamma_A^\infty(\pi_B)$ & $\gamma_B^\infty(\pi_A)$, $\gamma_B^\infty(\pi_A)$ & $\gamma_C^\infty(\pi_A)$, and $\gamma_B^\infty(\pi_C)$ & $\gamma_C^\infty(\pi_B)$. When this idea is extended to an *N*-component system, the number of unique pairs to that system becomes $N(N-1)/2$ and the number of infinite dilution activities to determine is $N(N-1)$.

From here, GPAST becomes a combinatorial and serial application of the PRAST system. Recall that in the PRAST method, a system of equations involving the activity model and the calculated infinite dilution activities is set up to solve for the parameters of the activity model for that binary system.[11] This same procedure is used in GPAST, but is applied sequentially over each binary set within the overall system, such that all of the activity model parameters for each pair of species can be determined.

To demonstrate this concept, consider Eqs. 10 and 11 from the SPD model to be the activity model chosen to describe the nonideal behavior at the surface of the adsorbent. To simplify this example, it will be assumed that the molecular shape factors (s_i) can be independently determined based on the adsorbing molecule size characteristics and that the only model parameters to be determined are the Boltzmann weighting factors: τ_{ij} and τ_{ji}. Then, continuing from the previous ternary example, a system of equations for each binary pair can be formulated as shown below in Eqs. 17–22

$$\lim_{\substack{x_A \to 0 \\ x_B \to 1}} (\ln\gamma_A) = \ln\gamma_A^\infty(\pi_B) = s_A(1-\ln\tau_{BA}-\tau_{AB}) \tag{17}$$

$$\lim_{\substack{x_B \to 0 \\ x_A \to 1}} (\ln\gamma_B) = \ln\gamma_B^\infty(\pi_A) = s_B(1-\ln\tau_{AB}-\tau_{BA}) \tag{18}$$

$$\lim_{\substack{x_A \to 0 \\ x_C \to 1}} (\ln\gamma_A) = \ln\gamma_A^\infty(\pi_C) = s_A(1-\ln\tau_{CA}-\tau_{AC}) \tag{19}$$

$$\lim_{\substack{x_C \to 0 \\ x_A \to 1}} (\ln\gamma_C) = \ln\gamma_C^\infty(\pi_A) = s_C(1-\ln\tau_{AC}-\tau_{CA}) \tag{20}$$

$$\lim_{\substack{x_B \to 0 \\ x_C \to 1}} (\ln\gamma_B) = \ln\gamma_B^\infty(\pi_C) = s_B(1-\ln\tau_{CB}-\tau_{BC}) \tag{21}$$

$$\lim_{\substack{x_C \to 0 \\ x_B \to 1}} (\ln\gamma_C) = \ln\gamma_C^\infty(\pi_B) = s_C(1-\ln\tau_{BC}-\tau_{CB}) \tag{22}$$

As the infinite dilution activities have already been calculated by Eq. 16, and the shape factors are independently determined, these equations represent a uniquely solvable, nonlinear system of six equations and six unknowns. Each τ_{ji} determined from these equations is then used back in the original activity model to represent the nonideality that occurs at the surface for the ternary system. From this point on, the standard AST system of equations (Eqs. 1–6) can be used to predict the adsorbed amounts in the system under various conditions of temperature and pressure, using the activity model with the parameters (τ_{ji}) calculated from GPAST.

It is important to note that GPAST is essentially a direct extension of the PRAST method with the purpose of generalizing the approach to be applicable to systems containing more than two adsorbable species. As such, if the number of adsorbable species in a system is only two, then GPAST is exactly the same as PRAST. However, GPAST has a clear advantage over PRAST in its ability to go beyond just a binary system and instead consider an *N*-component system.

Modified Spreading Pressure Dependency

It was shown previously that the SPD activity model proposed by Talu and Zwiebel[3] abides by the three thermodynamic criteria outline in Eqs. 7−9, which makes it a viable model to use for gas-solid adsorption. However, this model contains a set of three parameters (s_i, s_j, and β_{ij}) for each binary pair of adsorbing molecules (i and j). Note that the $\beta_{ij} = \beta_{ji}$ so that it only counts as one parameter instead of two. Therefore, the SPD model does not fit within the GPAST system because GPAST, like PRAST, requires that there be two parameters per binary pair in order for the resulting system of equations to be solvable.

Much like in the GPAST example considered previously, the SPD model can be initially modified by assuming the

shape factors are not model parameters, but instead are values which can be determined independently based on the characteristics of the adsorbing molecules. Bondi,[13] Abrams and Prausnitz,[8] and Vera et al.[14] proposed several methodologies for determining the shape factor of a molecule based on the van der Waals volume (v_i) of that molecule and the lattice coordination number (z), which is typically taken to be a constant. For simple, nonaromatic molecules, the shape factor (s_i) can be calculated simply from Eq. 23. Note that v^o is a constant that depends on the chosen coordination number. For a coordination number of 10, $v^o = 18.92$ cm^3/mole. Other values of v^o for various coordination numbers are tabulated in Vera et al.[14]

$$s_i = \frac{v_i(z-2)}{v^o z} + \frac{2}{z} \tag{23}$$

This relationship, or another similar method, may be used to eliminate the shape factors as parameters of the SPD model leaving β_{ij} as the only adjustable parameter. However, the GPAST system under these conditions still remains unsolvable because it needs the activity model to have exactly two parameters per binary pair. By having only one model parameter per binary pair, the system of equations is not uniquely solvable as there may be many values of that parameter that could minimize the residuals of the system, but not eliminate those residuals. Therefore, the SPD model must be further modified to fit into the GPAST system.

In the original SPD model, the β_{ij} parameter shows up in the equation for the lateral interaction potentials (e_{ij}) between molecules i and j (Eq. 14) and serves as a correction parameter for the geometric averaging of each molecules' interaction potential with itself (e_{ii}). However, this simple geometric average is only valid if both e_{ii} and e_{jj} have the same sign, positive or negative. This may not necessarily be the case as each adsorbing molecule is likely to have different energy characteristics with the surface loading and spreading pressure.

To correct this issue, a shifted geometric mean should be used for the lateral interaction potentials to eliminate the possible advent of imaginary numbers. In this type of averaging, the values being averaged are first shifted to the positive region of the domain by some factor such that all values underneath the square root are positive. Once the geometric average of the shifted values has been determined, the actual geometric average is back calculated out by undoing the initial shifting. A common use of this type of averaging is seen in financial economics in determination of the average rate-of-return (g) on an investment (Eq. 24). In this example, the shift factor is taken to be 1 (or 100%) for all returns (r_t) in a series of investments.[15] This equation can be generalized further by allowing the shift factor for each return to be any constant (C), such that the geometric mean then takes the form of Eq. 25

$$g = \sqrt[T]{\prod_t (1+r_t)} - 1 \tag{24}$$

$$g = \sqrt[T]{\prod_t (C+r_t)} - \mathrm{C} \tag{25}$$

Comparing Eqs. 25 to 14, it can be seen that the β_{ij} parameter of the activity model is essentially acting as a correction to the shift factor in the geometric mean. As such, we can redefine Eqs. 14 to 26 below using a shifted geometric mean of the interaction potentials (e_{ii}) and using a new correction parameter α_{ij} to replace the β_{ij} correction parameter used by Talu and Zwiebel.

$$e_{ji} = \sqrt{(\mu+e_{ii})(\mu+e_{jj})} - \alpha_{ji}\mu \tag{26}$$

$$\mu = \max\left\{ \max_{\forall \pi} |e_{ii}|, \max_{\forall \pi} |e_{jj}| \right\} \tag{27}$$

In this formulation, the variable μ is the maximum absolute value of the maximum of e_{ii} and e_{jj} at any spreading pressure (Eq. 27).

To stay consistent with the original SPD model, the correction parameters α_{ij} and α_{ji} must be equivalent. However, to fit within the GPAST system, there must be exactly two adjustable parameters per binary pair.To satisfy these two conditions, a simple mixing rule is adopted in which the lateral interaction potentials, through the new correction parameters, depend on the mole fractions (x_i) of the adsorbed molecules relative to the other adsorbing molecule for that particular binary pair as shown in Eqs. 28 and 29 below

$$\alpha_{ji} = (\eta_{ij} - \eta_{ji})\left(\frac{x_j}{x_i + x_j}\right) + \eta_{ji} \tag{28}$$

$$\alpha_{ij} = (\eta_{ji} - \eta_{ij})\left(\frac{x_i}{x_i + x_j}\right) + \eta_{ij} \tag{29}$$

From this relationship, it can be shown that $\alpha_{ij} = \alpha_{ji}$ for any values of x_i and x_j and is therefore consistent with the original SPD model and contains two adjustable parameters (η_{ij} and η_{ji}) per binary pair.

The MSPD model replaces Eq. 14 from the original SPD model with Eqs. 26 through 29 outlined above. These modifications still maintain the overall significance and behavior of the original SPD model, but allow it to fit within the GPAST system by having exactly two adjustable parameters. Additionally, much like the original SPD model, the MSPD model maintains the three criteria shown in Eqs. 7–9 above, making it a thermodynamically consistent model. When the MSPD model is combined with the GPAST system and the original six equations from AST (Eqs. 1–6), a closed system of equations can be developed in which one can predict the nonidealities and adsorbed amounts of an N-component system under various conditions of pressure and temperature.

Pure Component Isotherm Considerations

The final step to consider before solving the resulting system of equations is the form of the pure component isotherm model that appears in Eq. 6 of the AST system. This model can technically take any form, as long as the pure adsorbed amount (q_i^o) can be expressed as an explicit function of the pure gas partial pressure (p_i^o). However, there are a few thermodynamic considerations to reflect on prior to choosing a particular isotherm model.

One major criterion for the isotherm model is that it must obey Henry's law at low pressure. This is required not only by the GPAST system (Eqs. 15 and 16), but is also necessary for the evaluation of the spreading pressure in AST (Eq. 1). The most common isotherm model that obeys this behavior is the Langmuir isotherm (Eq. 30). However, this model is somewhat limited in its ability to describe a wide variety of pure gas adsorption data and is theoretically only applicable to homogenous adsorbent surfaces. For the GPAST

system, a more general isotherm model that can be applicable to homogeneous and heterogeneous surfaces may be more desirable

$$q_i^o = q_{\max,i}\frac{K_i p_i^o}{1+K_i p_i^o} \tag{30}$$

Llano-Restrepo and Mosquera[16] discuss the derivation of a generalized statistical thermodynamic adsorption (GSTA) isotherm model, shown in Eq. 31, which is based on Hill's statistical equilibrium model.

$$q_i^o = \frac{q_{\max,i}}{m_i}\frac{\sum_{n=1}^{m_i} nK_{n,i}^o\left(p_i^o/P^o\right)^n}{1+\sum_{n=1}^{m_i} K_{n,i}^o\left(p_i^o/P^o\right)^n} \tag{31}$$

$$\ln K_{n,i}^o = -\frac{\Delta H_{n,i}^o}{RT}+\frac{\Delta S_{n,i}^o}{R} \tag{32}$$

This model considers the adsorbed phase to be an ensemble of subsystems that are all energetically distinct from each other (i.e., surface sites of various energy characteristics). The primary difference between the GSTA model and Hill's model is that there is a physically significant correlation between the GSTA model and the Heterogeneous Langmuir model.[17] In the GSTA model, the parameters of $q_{\max,i}$ and m_i represent the theoretical maximum adsorption capacity and number of energetically distinct adsorption sites, respectively, and the K_n^o parameters are the dimensionless equilibrium constants associated with each adsorption site.[16] These equilibrium constants are then related to temperature (T), enthalpy (ΔH), and entropy (ΔS) through the van't Hoff expression in Eq. 32. Note that P^o is the standard state pressure, typically taken to be 100 kPa.

The advantage of using this isotherm model is that it can account for both surface homogeneity, as well as heterogeneity, depending on the surface characteristics of the particular adsorbent. Under the condition that there is only one type of adsorption site ($m_i = 1$), this model reverts down to the standard Langmuir model. Additionally, as this model has many adjustable equilibrium parameters, it has the potential to describe a wide variety of different pure species isotherms. Llano-Restrepo and Mosquera[16] have also derived an expression for the isosteric heat of adsorption (Eq. 33) as a function of the loading ($\varphi_i = q_i^o/q_{\max,i}$) of the adsorbent, which is needed for determining the interaction potentials (e_{ii}) of the MSPD model (Eq. 13).

$$Q_i^{st} = \frac{\sum_{n=1}^{m_i}(m_i\varphi_i - n)K_{n,i}^o\left(p_i^o/P^o\right)^n\left(-\Delta H_{n,i}^o\right)}{\sum_{n=1}^{m_i}(m_i\varphi_i - n)nK_{n,i}^o\left(p_i^o/P^o\right)^n} \tag{33}$$

Application of GPAST with MSPD and GSTA

The culmination of the GPAST system together with the MSPD activity model and GSTA isotherm creates a fully closed, solvable, nonlinear system of equations for which one can predict the nonideal adsorption behavior of a mixed gas system containing any number of adsorbable components. However, this system has become significantly more involved than AST and will require a comprehensive software code to handle these added complexities. The code developed here performs a series of stepwise actions to setup the system and solve for either the adsorbed phase or gas phase composition of the mixed system depending on what information it is initially supplied with. This software is referred to as the multicomponent adsorption generalized procedure for isothermal equilibria or MAGPIE for short.

Prior to the development and execution of MAGPIE, the GPAST system can be simplified by forming an analytical solution to the evaluation of the spreading pressure in Eq. 1. To quantify this integral requires use of the isotherm expression, which in this case is the GSTA model (Eq. 31). The analytical solution to this integral can be obtained by use of a simple substitution technique, which results in the expression below in Eq. 34. Additionally, the values of the Henry's law constant (He_i) for the GSTA isotherm can be formulated as in Eq. 35, such that these limits do not need to be estimated numerically in the software routines

$$\Pi = \frac{q_{\max,i}}{m_i}\ln\left(1+\sum_{n=1}^{m_i} K_{n,i}^o\left(p_i^o/P^o\right)^n\right) \tag{34}$$

$$He_i = \frac{q_{\max,i}K_{1,i}^o}{m_i P^o} \tag{35}$$

Before MAGPIE can evaluate the GPAST system of equations, each infinite dilution activity for each unique binary pair of species in the overall system must be determined by Eq. 16. This is accomplished by recognizing that the spreading pressure of the system, under infinite dilution conditions, is only being contributed to by the component whose adsorbed mole fraction is unity ($x_j = 1$). Additionally, from Eq. 7, the activity of that component must also be unity ($\gamma_j = 1$). Therefore, from Eq. 2, the reference state pressure for that component (p_j^o) is exactly equal to the partial pressure of that component in the gas phase ($P_T y_j$).

Using that reference state pressure for the jth component, MAGPIE can solve directly for the spreading pressure at infinite dilution (π_j) using Eq. 34 and the reference amount adsorbed (q_j^o) with Eq. 31. Then, because the spreading pressure of the system must be equivalent for all species in the mixture, MAGPIE solves for the reference state pressure of the ith component at the jth spreading pressure, $p_i^o(\pi_j)$, using Eq. 34. However, the solution at this particular step requires a nonlinear, iterative technique because the variables are not separable.

After these steps are completed, MAGPIE can directly calculate the infinite dilution activities of the system for each binary pair. That information is stored and used in the GPAST system of equations to determine the interaction parameters (η_{ij} and η_{ji}) of the MSPD model in a similar fashion to the GPAST example shown in Eqs. 17–22. However, for this particular application, the τ_{ij} and τ_{ji} parameters from Eqs. 17−22 would be replaced with their actual expressions in the MSPD model, such that the parameters being solved for in this system are the interaction parameters (η_{ij} and η_{ji}). This step also requires the use of a nonlinear, iterative solver.

After the interaction parameters (η_{ij} and η_{ji}) of MSPD have been calculated and stored, they can then be used to solve the AST system (Eqs. 1–6) without neglecting the activity coefficients. Again, this step requires a nonlinear, iterative technique. The solution to this final system of equations will yield the predicted adsorbed amounts for each adsorbable species as well as the total amount being adsorbed. Evaluation of the gradient of activity to spreading pressure in Eq. 3 is performed numerically using a centered difference approach for second-order accuracy (Eq. 36). An analytical solution to this derivative cannot be formed because the activity is an implicit function of spreading pressure in the MSPD model.

$$\frac{\partial \ln\gamma_i}{\partial \Pi} = \frac{\ln\gamma_i(\Pi+\Delta\Pi) - \ln\gamma_i(\Pi-\Delta\Pi)}{2\Delta\Pi} + O(\Delta\Pi^2) \tag{36}$$

Many of the steps involved in solving this system require the use of a nonlinear solver. To accommodate this need, MAGPIE makes use of a small, standalone C library called *lmfit*,[18] which is used to solve nonlinear systems of equations using a Levenberg–Marquardt algorithm. This library has demonstrated respectable convergence over a variety of test cases and is used throughout MAGPIE for all nonlinear systems.

A Special Case of the MAGPIE Application

Because the MAGPIE application is the culmination of the GPAST system with the GSTA isotherm and MSPD activity model, there is a special circumstance under which this application will revert down to the extended Langmuir model for multicomponent adsorption. To demonstrate this, consider a binary gas system composed of molecules A and B, with the pure gas isotherms of both species being described by the GSTA model. Additionally, if the isotherms are homogenous in form (i.e., $m_A = 1$ and $m_B = 1$), then the GSTA model itself reverts to the standard Langmuir model for both species (Eqs. 37 and 38).

$$q_A^o = \frac{q_{\max,A} K_{1,A}^o \left(p_A^o/P^o\right)}{1 + K_{1,A}^o \left(p_A^o/P^o\right)} \tag{37}$$

$$q_B^o = \frac{q_{\max,B} K_{1,B}^o \left(p_B^o/P^o\right)}{1 + K_{1,B}^o \left(p_B^o/P^o\right)} \tag{38}$$

By considering the equation for isosteric heat of adsorption (Eq. 33) derived for the GSTA isotherm, it can be shown that, under the homogeneous case, this energy term is equivalent to the enthalpy[16] (Eq. 39). Therefore, for molecules A and B, the isosteric heat Q_i^{st} would not be changing with the spreading pressure. That being the case, the lateral interaction parameters (e_{AB}, e_{AA}, and e_{BB}) from MSPD will all be zero, which in turn causes all the Boltzmann weighting factors (τ_{AB} and τ_{BA}) to become one. If all of these weighting factors are always one, then the activity for each adsorbing species will always be unity ($\gamma_A = 1$ and $\gamma_B = 1$).

$$Q_i^{\text{st}}|_{m_i=1} = \left(-\Delta H_{1,i}^o\right) \tag{39}$$

Under these exact circumstances, the GPAST system will revert down to IAST. In addition, as the GSTA isotherm for molecules A and B both take the form of the Langmuir equation, the IAST system of equations can then be solved analytically, instead of numerically. The solution to IAST when all isotherms obey the Langmuir model results in the standard extended Langmuir model (Eq. 40). This conclusion could also be obtained qualitatively by reasoning that the primary assumption behind the extended Langmuir model is that the different adsorbate molecules do not interact with each other,[4] which was determined in the MSPD model for this case by having all the lateral interaction potentials (e_{ij}) equal to zero.

$$q_i = \frac{q_{\max,i} K_{1,i}^o (p_i/P^o)}{1 + \sum_{j=1}^{N} K_{1,j}^o \left(p_j/P^o\right)} \tag{40}$$

Results and Comparison with IAST

To quantify the predictive capabilities of MAGPIE requires use of actual multicomponent adsorption data, either obtained experimentally or found in literature. Two sets of adsorption data available in literature will serve as test cases for MAGPIE: (i) Talu and Zwiebel data for binary and ternary mixtures of CO_2, H_2S, and C_3H_8 on an H-mordentite adsorbent[3] and (ii) Ritter and Yang data for various mixtures of CH_4, CO_2, CO, H_2, and H_2S on activated carbon.[19] The results of MAGPIE will then be compared against the results of IAST for the same data sets. It is expected that MAGPIE will show a significant improvement in predictive capabilities over IAST.

To eliminate as much bias in the analysis as possible, both MAGPIE and IAST will use the GSTA model for the pure component isotherms. Therefore, the only differences in the system of equations will be the activity model and the GPAST procedure used to adjust that model to the infinite dilution activities. After the GSTA model has been calibrated to each set of single component data, the parameters of that model can be used in the evaluation of both the MAGPIE and IAST system.

The comparison between MAGPIE and IAST will be examined by studying the differences in the distribution of error between each numerical result and the actual data. There are two predicted quantities to be compared from MAGPIE and IAST: (i) the adsorbed mole fractions (x_i) and (ii) the total amount adsorbed (q_T), of which there are 214 and 86 observations, respectively. Because the adsorbed mole fractions are a bounded quantity (Eq. 4), the errors associated with predicting those values will be determined as an absolute difference (absolute error = predicted—actual). However, the total amount adsorbed is unbounded, so its error will be quantified in terms of a relative difference (relative error = [predicted—actual]/actual), which would be analogous to a percent error in this quantity.

These errors are formulated such that a positive error represents an overestimate, while a negative error reflects an underestimate. This allows us to show how the error is distributed and where any error bias may occur. However, these error distributions would not capture total error, as any positive error could be offset by an equal negative error. Therefore, we will also compare the average Euclidean errors (E_{avg}) of both predicted quantities (x_i and q_T) for each method (MAGPIE and IAST) by taking the square root of the sum of the squares of the errors divided by the number of observations made (M).

$$E_{\text{avg}} = \frac{1}{M}\sqrt{\sum_{i=1}^{M} \left(\text{predicted}_i - \text{actual}_i\right)^2} \tag{41}$$

Results for the errors in adsorbed mole fractions can be seen in the histogram on Figure 1. The size of each bin in the histogram is 0.05 in absolute error and each bin is named after its median error for that bin (i.e., bin 0.025 ranges from 0 to 0.05 in absolute error). At a glance, it can be seen from this figure that MAGPIE has a relatively standard distribution of error, but IAST appears to have two-outer peaks at bins −0.175 and 0.175. These particular error bins are being filled mostly from IAST errors associated with predicting the Talu and Zwiebel data, but cannot be pinpointed to any particular mixture or species.

Additionally, both MAGPIE and IAST errors follow roughly a normal-type distribution centered near zero error. However, MAGPIE appears to have a greater number of results occurring closer to zero than IAST. Note that in reality neither MAGPIE nor IAST can have a normal

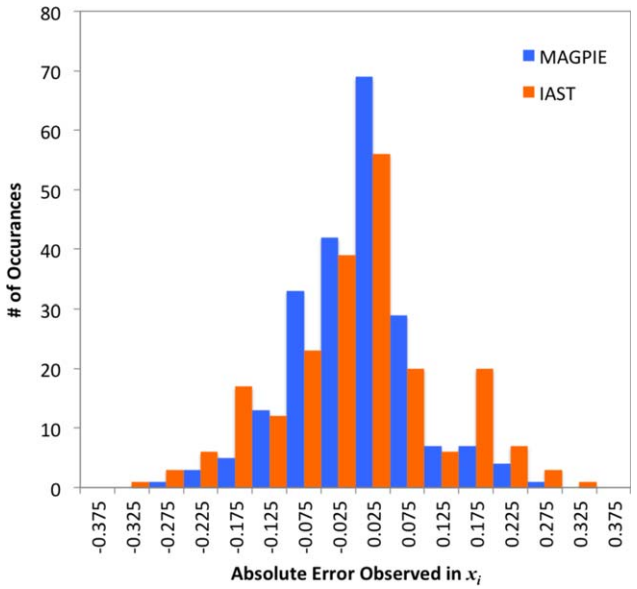

Figure 1. Error distribution histogram for the absolute errors observed in the adsorbed mole fractions predicted from both MAGPIE and IAST.

[Color figure can be viewed in the online issue, which is available at wileyonlinelibrary.com.]

distribution of absolute error for this observation because it is a bounded observation wherein the maximum errors are ± 1. A real normal distribution is an unbounded observation, so we are idealizing the error distribution of MAGPIE and IAST as a normal distribution to more easily study the error quantitatively.

For the total adsorbed amounts (Figure 2), the distribution is much wider spread. Here, the bin sizes are 0.05 in relative error and each bin is again named after its median error. Immediately apparent is what appears to be a large outlying peak for MAGPIE errors in bin 0.125. Nearly all (8 out of 11) of these error observations come from a single mixture in the Talu and Zwiebel data set: CO_2 and H_2S on H-mordenite. Both CO_2 and H_2S show very high affinity toward H-mordenite, from their single component isotherms, and are highly polar molecules,[3] which may contribute to the overestimations in the adsorption capacities for this mixture.

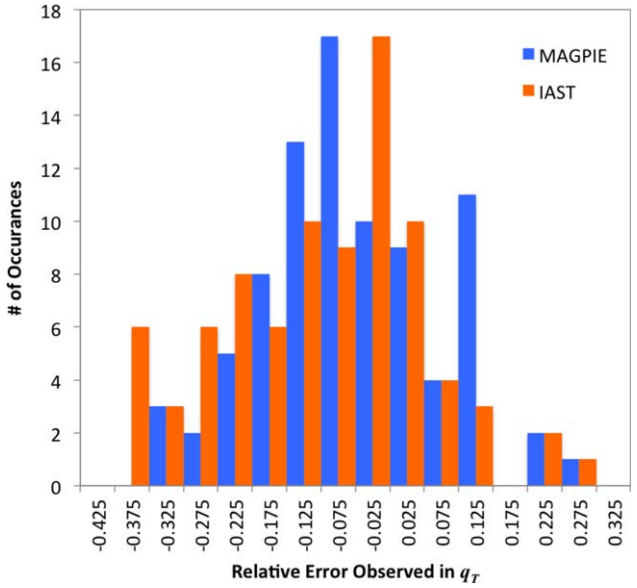

Figure 2. Error distribution histogram for the relative errors observed in the adsorbed totals predicted from both MAGPIE and IAST.

[Color figure can be viewed in the online issue, which is available at wileyonlinelibrary.com.]

Looking at Figure 2 it is difficult to determine precisely which methodology has produced better results. Unlike the fairly standard distributions of error observed from Figure 1, Figure 2 appears to be more irregular in shape with little peaks and valleys moving from left to right, especially for IAST. However, overall the general trends observed do create the bell shaped curve we expect to see for distributions of random variables. To precisely determine which method has resulted in a better distribution of error, a more quantitative analysis will be necessary, but it can at least be seen from this figure that both MAGPIE and IAST show a slight negative bias in the errors. This means that both methods, on average, have predicted adsorbed amounts lower than the actual measured data.

To compare the performance between MAGPIE and IAST, a statistical analysis is performed on the error distributions from Figures 1 and 2. For this analysis, we will idealize these actual error distributions as normal distributions and quantify properties such as average values and standard deviations, which can be used to plot probability density functions associated with each error histogram. Each histogram is first normalized using the observations of each bin and the total number of observations such that the total area underneath each corresponding probability density function will be 1. Then, from those normalized curves, we approximated the average values and standard deviations of each distribution of observations. It is desired that MAGPIE show reduction in both the average error bias and error standard deviation for both predicted quantities.

Table 1 summarizes the results of this analysis. For the errors in adsorbed mole fractions, MAGPIE showed no improvement in the average error bias. However, both MAGPIE and IAST had almost no error bias in this quantity, which is primarily attributed to the bounding of the mole fractions (Eq. 4). Due to this bounding, any negative error in adsorbed amount x_j would be offset by an equal positive error in x_i, such that the sum of all mole fractions equals one. As such, there is not expected to be any error bias in this average quantity to begin with.

In all other regards, Table1 demonstrations that MAGPIE results show dramatic improvement over IAST. There was a 36% reduction in the standard deviation of the absolute error in the adsorbed mole fractions, meaning that the MAGPIE predictions of this quantity are grouped more closely around the actual data than IAST results. Additionally, MAGPIE shows a near 28% reduction in the average Euclidean error of the mole fractions, which indicates that the magnitude of

Table 1. Summary of the Statistical Analysis of the Error

	MAGPIE	IAST	Improvement (%)
Absolute error of mole fractions			
Average	0.001	0.001	0.00
Standard deviation	0.062	0.097	−36.14
E_{avg} (Eq. 41)	5.76E-3	7.98E-3	−27.87
Relative error of adsorbed totals			
Average	−0.048	−0.092	−48.43
Standard deviation	0.114	0.139	−17.72
E_{avg} (Eq. 41)	0.050	0.053	−5.26

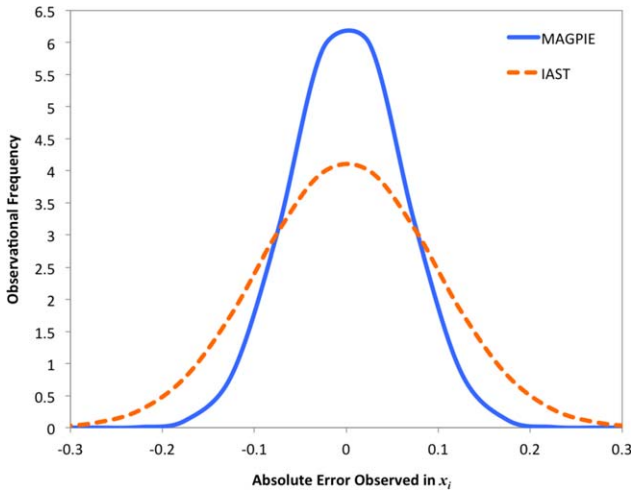

Figure 3. Idealized normal probability density functions for the absolute error in the adsorbed mole fractions generated from the averages and standard deviations of Table 1 that were based on the statistical analysis of the error histograms from Figure 1.

[Color figure can be viewed in the online issue, which is available at wileyonlinelibrary.com.]

the errors observed from MAGPIE were on average 28% smaller than those observed for IAST.

For the adsorbed totals, both IAST and MAGPIE still showed a tendency to underestimate adsorption, as indicated by the negative values for average error, but MAGPIE showed a resounding 48% reduction in that negative error basis. This means that, on average, MAGPIE results were significantly closer to the real adsorption totals compared with the IAST results. However, the standard deviations of these errors were relatively similar, 0.114 for MAGPIE compared with 0.139 for IAST, which resulted in the average Euclidean errors being very similar, 0.050 for MAGPIE compared with 0.053 for IAST. In both cases, MAGPIE did yield better results, but the gains were marginal, roughly 18% improvement in standard deviations and only a 5% improvement in average Euclidean error.

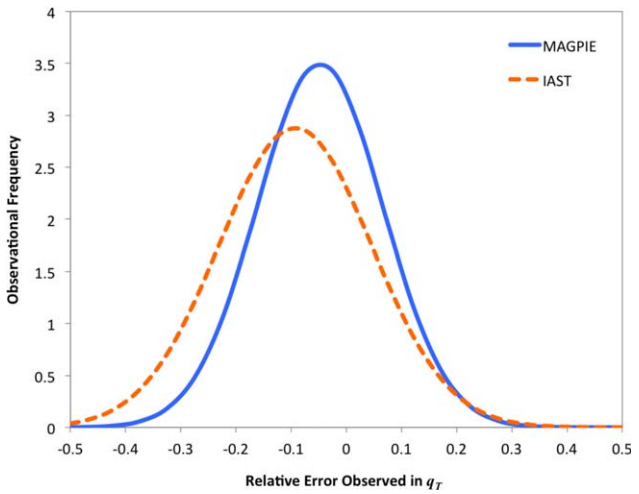

Figure 4. Idealized normal probability density functions for the relative error in the adsorbed totals generated from the averages and standard deviations of Table 1 that were based on the statistical analysis of the error histograms from Figure 2.

[Color figure can be viewed in the online issue, which is available at wileyonlinelibrary.com.]

To visualize this information, the average and standard deviations from Table 1 are used to plot probability density functions for each distribution of error in Figures 3 and 4. These plots show the dramatic difference in the idealized error distributions between MAGPIE and IAST. In both figures, MAGPIE error is grouped more tightly around the average as a result of the reduction in the standard deviation for both distributions. For Figure 4, MAGPIE also shows a shift in the average error toward zero error, which demonstrates a reduction in the negative bias of the adsorbed totals found in IAST. These results demonstrate that MAGPIE results have dramatically improved over the results of IAST for the same data set.

Discussion

The actual MAGPIE results and literature data are plotted in Figures 5 and 6 for the adsorbed mole fractions and in Figures 7 and 8 for the adsorption totals. In these plots, the solid lines represent the equivalence line at which the result from the MAGPIE simulation (y axis) is exactly equal to the measured value recorded in literature (x axis). The dashed lines show the boundaries, determined by the statistical analysis, in which 95% of all points lay between (i.e., $\pm$ twice the standard deviations). Note that the dashed lines for Figures 5 and 6 are parallel while the dashed lines fan outward for Figures 7 and 8. This is because the error distribution analyzed for the adsorbed mole fractions was done in terms of an absolute error (Figure 1), but the error distribution for adsorption totals was performed on the relative error (Figure 2).

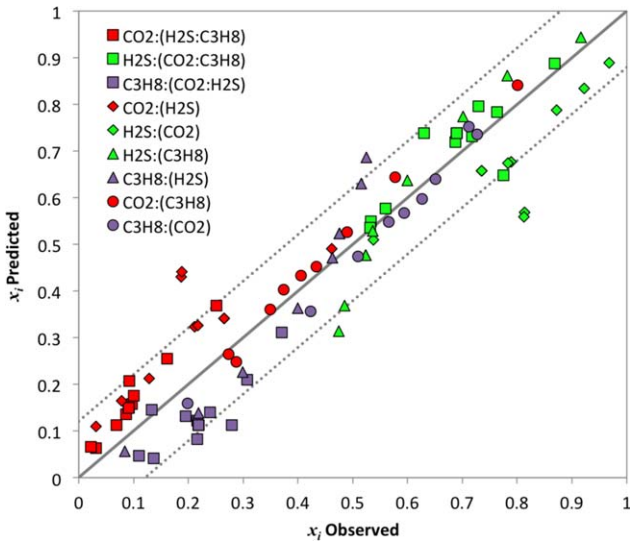

Figure 5. MAGPIE results vs. the Talu and Zwiebel[3] reported adsorbed mole fractions.

Solid line represents the equivalence line between model and data, while the dashed lines show the 95% confidence intervals based on the statistical analysis. The different mixtures each has its own symbol and is labeled by which species is being observed, followed by the other species involved in the mixture in parentheses. Different colors are also used to denote which species is being observed (i.e., red = CO_2, green = H_2S, and purple = C_3H_8). [Color figure can be viewed in the online issue, which is available at wileyonlinelibrary.com.]

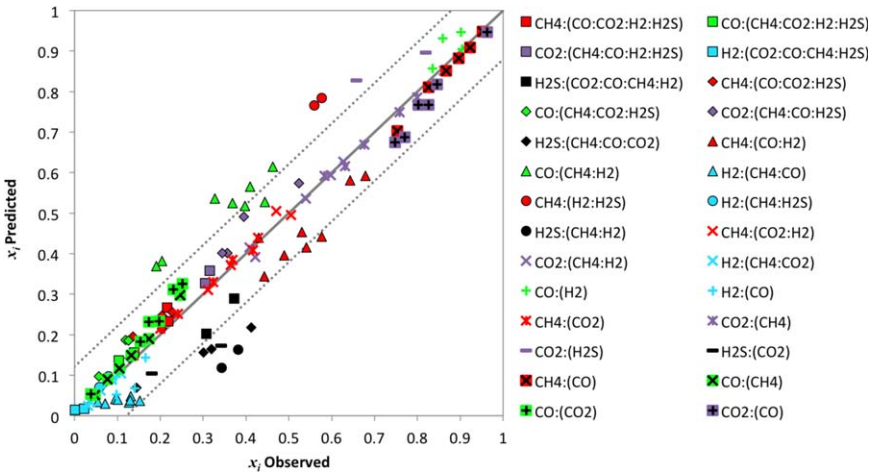

Figure 6. MAGPIE results vs. the Ritter and Yang[19] reported adsorbed mole fractions.

Solid line represents the equivalence line between model and data, while the dashed lines show the 95% confidence intervals based on the statistical analysis. The different mixtures each has its own symbol and is labeled by which species is being observed, followed by the other species involved in the mixture in parentheses. Different colors are also used to denote which species is being observed (i.e., red = CH_4, green = CO, purple = CO_2, blue = H_2, and black = H_2S). [Color figure can be viewed in the online issue, which is available at wileyonlinelibrary.com.]

The results shown in Figures 5 and 6 generally show very good agreement with the observations made by Talu and Zwiebel[3] and Ritter and Yang.[19] However, there are some notable outliers in both sets of results. For instance, in Figure 5 it can be seen that MAGPIE has consistently overestimated the CO_2 adsorbed mole fractions (red diamonds) and underestimated the H_2S mole fractions (green diamonds) for the binary mixtures. This may be caused by the highly polar nature of these two species, which is a factor that the activity model does not take into account. Also in Figure 5, for the ternary mixtures of CO_2, H_2S, and C_3H_8, the mole fractions of H_2S (green squares) are very close to the equivalent line, while CO_2 (red squares) is consistently overestimated and C_3H_8 (purple squares) consistently underestimated. This is most likely a result of the relative adsorption strengths of CO_2 and C_3H_8. CO_2 has a much higher affinity to adsorb to the H-mordenite than the C_3H_8[3] and therefore would be expected to show a larger mole fraction than C_3H_8 in the adsorbed phase.

Figure 6 showed fewer outliers than Figure 5, but still had some points and species that were consistently outside of the expected values. Most notable of those species was H_2S (all black shapes), whose mole fractions were underestimated by MAGPIE for nearly all mixtures and experiments. It is unclear as to why this is compared with what was seen in Figure 5,

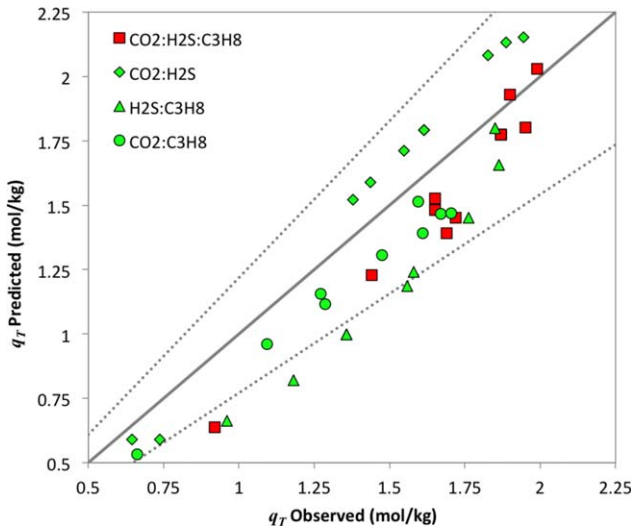

Figure 7. MAGPIE results vs. the Talu and Zwiebel[3] reported adsorbed totals.

Solid line represents the equivalence line between model and data, while the dashed lines show the 95% confidence intervals based on the statistical analysis. Each symbol denotes a different mixture and those same symbols correspond to the mixtures in Figure 5. Colors identify whether the mixture is binary, ternary, and so forth. (i.e., red = ternary and green = binary). [Color figure can be viewed in the online issue, which is available at wileyonlinelibrary.com.]

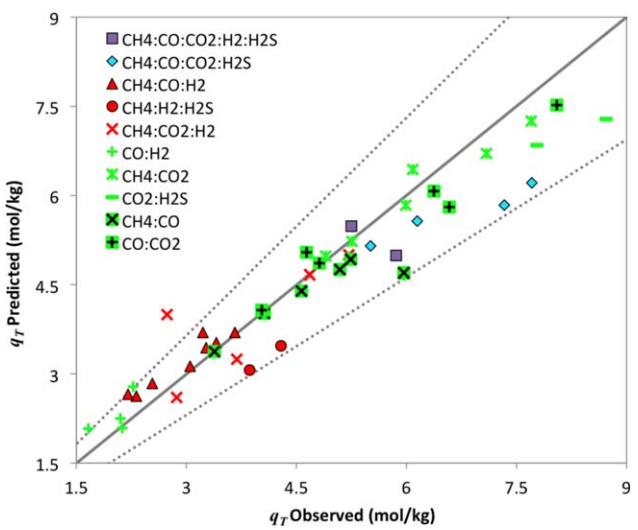

Figure 8. MAGPIE results vs. the Ritter and Yang[19] reported adsorbed totals.

Solid line represents the equivalence line between model and data, while the dashed lines show the 95% confidence intervals based on the statistical analysis. Each symbol denotes a different mixture and those same symbols correspond to the mixtures in Figure 6. Colors identify whether the mixture is binary, ternary, and so forth. (i.e., purple = quinary, blue = quaternary, red = ternary, and green = binary). [Color figure can be viewed in the online issue, which is available at wileyonlinelibrary.com.]

because the mixtures for the Ritter and Yang[19] data are much more varied. However, many of those mixtures do involve other polar components (CO and CO_2), which themselves are usually being overestimated (green triangles and purple dashes). Based on the consistency of these observations, an improvement to MAGPIE could be made by including factors for polarization of species in the activity model.

Figures 7 and 8 also generally show good agreement with the adsorption totals observed from the Talu and Zwiebel[3] and Ritter and Yang[19] data sets. However, both sets of results show a negative bias, or a tendency for MAGPIE to underestimate the adsorption. This observation is especially true in the case of the Talu and Zwiebel[3] data set (Figure 7), which shows a negative bias for all mixtures except the CO_2 and H_2S mixtures. For that particular mixture, MAGPIE consistently overestimates the adsorption capacities by roughly 10%. This is the same mixture that caused the overestimations and underestimations in the adsorbed mole fractions of Figure 5 so it is likely that these overestimations could also be attributed to the polarity of CO_2 and H_2S. The other mixtures from Figure 7 show a negative bias, which could be attributed to the low affinity of adsorption for C_3H_8 on H-mordenite,[3] as all other mixtures involve this species.

The adsorption capacity results in Figure 8 for the Ritter and Yang[19] data show much better agreement than the results for the Talu and Zwiebel[3] data. In fact, MAGPIE shows almost no negative bias for these data sets as the majority of results are spread nearly equally around the equivalence line. The exceptions would be the quaternary mixture (blue diamonds) and the CO_2 and H_2S binary mixture (green dashes), which both show a consistent negative bias in the results. Each of these mixtures also contain all, or a majority, of polar species in the adsorbed phase.

Conclusions

The results from the above analysis indicate that MAGPIE has demonstrated a significant improvement in predictive capabilities over IAST for the data sample given. However, it is important to note that MAGPIE is only a single application of GPAST and these results may have been different if another isotherm or activity model were used in place of the GSTA and MSPD models. Recall that GPAST itself only requires that the isotherm abide by Henry's law (Eq. 15) and that the activity model obey a set of thermodynamic criteria (Eqs. 7−9) while containing two-adjustable parameters per binary pair, which are to be determined by the GPAST procedure. This means that it is possible to use any other isotherm or activity model that is found to be applicable, making GPAST a very generalized and flexible technique. It is this tremendous flexibility that makes GPAST such a powerful analytical tool for multicomponent adsorption equilibria.

Additionally, unlike its predecessor PRAST, GPAST is not limited to analyzing only binary adsorption systems. As was demonstrated with the Talu and Zwiebel[3] and Ritter and Yang[19] literature data, GPAST can be used to model and predict binary, ternary, quaternary, quinary, and larger adsorption systems. The generalization of the PRAST to GPAST is performed in a combinatorial and serial fashion, such that it can apply to any number of adsorbable components in a mixture, thus, further adding to the flexibility of GPAST.

Another advantage of GPAST is that this procedure does not require any calibration with binary adsorption data. It is a fully predictive model in which solutions to the adsorbed phase are determined by using only the adsorption behavior of each individual species in the mixture. The predictions being made are also fully reversible as the system of equations is deterministic. Therefore, when given a specific gas phase composition A, the adsorbed phase solution will be B, and if given a specific adsorbed phase composition B, the gas phase solution will be A.

Due to the apparent flexibility of GPAST, it would be very simple to further extend on this procedure to produce new applications simply by adding, removing, or changing the isotherm and activity models. MAGPIE was only one example of an application built on the GPAST procedure. With dozens of different isotherm and activity models available in literature, there are potentially hundreds of different applications of GPAST that could be developed and utilized for predicting thousands of different adsorption systems.

Notation

A = specific surface area of adsorbent, m^2/kg
C = shift factor in the geometric mean
e = lateral interaction potential, J/mol
E_{avg} = average Euclidean errors of predictions
$f(x)$ = variable f as a function of variable x
g = geometric mean of a sample
He = Henry's law constant, mol/kg/kPa
K = equilibrium constant, 1/kPa
K^o = dimensionless equilibrium constant
m = number of energetically distinct adsorption sites in GSTA
M = number of observations or data points
N = number of adsorbable species in a mixture
O = mathematical error term or truncation error
p = partial or reference state pressure, kPa
P = total or standard state pressure, kPa
q = adsorbed amount, mol/kg
Q^{st} = isosteric heat of adsorption, J/mol
R = ideal gas law constant, J/K/mol
r = return on investment
s = molecular shape factor
T = sample size for the geometric mean
v = van der Waals volume of a molecule, cm^3/mol
x = adsorbed mole fraction
y = gas phase mole fraction
z = coordination number of adsorbed phase lattice

Greek letters

α = lateral interaction potential correction parameter of MSPD
β = geometric mean correction parameter of SPD
γ = activity coefficient of the adsorbed phase
ΔH = enthalpy of adsorption, J/mol
ΔS = entropy of adsorption, J/K/mol
η = binary interaction parameter of MSPD
θ = external contact fraction of molecules in adsorbed phase
μ = maximum lateral interaction potential, J/mol
Π = lumped spreading pressure term, mol/kg
π = spreading pressure of adsorbed phase, J/m^2
τ = Boltzmann weighting factor
φ = fractional adsorption loading

Sub/superscripts

∞ = infinite dilution
i,j,k = indices for adsorbable species
max = maximum adsorption capacity
n = index of adsorption site
o = standard or reference state
T = total amount of some value
t = index of investment returns

Abbreviations

AST = adsorbed solution theory
GPAST = generalized predictive adsorbed solution theory
GSTA = generalized statistical thermodynamic adsorption

IAST = ideal adsorbed solution theory
MAGPIE = multicomponent adsorption generalized procedure for isothermal equilibria
MSPD = modified spreading pressure dependent
PRAST = predictive real adsorbed solution theory
SPD = spreading pressure dependent

Acknowledgment

Research was performed using funding received from the US DOE Office of Nuclear Energy's Nuclear Energy University Program (Grant # NFE-12-03822).

Literature Cited

1. Myers AL, Prausnitz JM. Thermodynamics of mixed-gas adsorption. *AIChE J*. 1965;34:121–127.
2. Talu O, Myers AL. Rigorous thermodynamic treatment of gas adsorption. *AIChE J*. 1988;34:1887–1893.
3. Talu O, Zwiebel I. Multicomponent adsorption equilibria of nonideal mixtures. *AIChE J*. 1986;32:1263–1276.
4. Tien C. Adsorption Calculations and Modeling. Newton, MA: Butterworth-Heinemann, 1994.
5. Myers AL. Activity coefficients of mixtures adsorbed on heterogeneous surfaces. *AIChE J*. 1983;29:691–693.
6. Cochran TW, Kabel RL, Danner RP. Vacancy solution theory of adsorption using Flory-Huggins activity coefficient equations. *AIChE J*. 1985;31:268–277.
7. Costa E, Sotelo JL, Calleja G, Marron C. Adsorption of binary and ternary hydrocarbon gas mixtures on activated carbon. *AIChE J*. 1981;27:5–12.
8. Abrams DS, Prausnitz JM. Statistical thermodynamics of liquid mixtures. *AIChE J*. 1975;21:116–128.
9. Maurer G, Prausnitz JM. On the derivation and extension of the UNIQUAC equation. *Fluid Phase Equilib*. 1978;2:91–99.
10. Fredenslund A, Jones RL, Prausnitz JM. Group contribution estimation of activity coefficients in nonideal liquid mixtures. *AIChE J*. 1975;21:1086–1099.
11. Sakuth M, Meyer J, Gmehling J. Measurement and prediction of binary adsorption equilibria of vapors on dealuminated Y-zeolites. *Chem Eng Process*. 1998;37:267–277.
12. Tondeur D, Yu F, Bonnot K, Luo L. Modeling spreading-pressure-dependent binary gas coadsorption equilibria using gravimetric data. *J Colloid Interface Sci*. 2006;293:342–352.
13. Bondi A. Van der Waals volumes and radii. *J Phys Chem*. 1964;68:441–451.
14. Vera JH, Sayegh SG, Ratcliff GA. A quasi lattice-local composition model for the excess Gibbs free energy of liquid mixtures. *Fluid Phase Equilib*. 1977;1:113–135.
15. Markowitz H. Mean-variance approximations to the geometric mean. *Ann Financ Econ*. 2012;7:1–30.
16. Llano-Restrepo M, Mosquera MA. Accurate correlation, thermochemistry, and structural interpretation of equilibrium adsorption isotherms of water vapor in zeolite 3a by means of a generalized statistical thermodynamic adsorption model. *Fluid Phase Equilib*. 2009;283:73–88.
17. Ladshaw A, Yiacoumi S, Tsouris C, DePaoli D. Generalized gas-solid adsorption modeling: single-component equilibria. *Fluid Phase Equilib*. 2015;388:169–181.
18. Wuttke J. lmfit—a C library for Levenberg-Marquardt least-squares minimization and curve fitting. Version <lmfit-3.4>. Available at: http://apps.jcns.fz-juelich.de/doku/sc/lmfit. Accessed January 21, 2013.
19. Ritter JA, Yang RT. Equilibrium adsorption of multicomponent gas mixtures at elevated pressures. *Ind Eng Chem Res*. 1987;26:1679–1686.

Manuscript received Sep. 2, 2014, and revision received Mar. 27, 2015.